VOLUME 1, 2018
DOI: 10.31058/j.ap.2018.11001

Synthesis and Variation Studies for the Magnetic Properties of $TM_{0.15}Co_{0.1}Zn_{0.75}O$ (TM= Ni, Mn)

Sabiu Said Abdullahi[1]*, Abdussalam B. Suleiman[1], Yuksel Koseoglu[2], Yusuf Shehu[3], Yasin Celaleddin Durmaz[4], Ibrahim M. Musa[1], Haidar Masud Alfanda[5]

[1] Physics Department, Federal University Dutse, Dutse, Jigawa State, Nigeria
[2] Department of Primary Education, Faculty of Education, Suleyman Demirel University, Cunur, Isparta, Turkey
[3] Department of Physics, Kano University of Science and Technology, Wudil Kano State, Nigeria
[4] Department of Physics, Bilkent University, Bilkent, Ankara, Turkey
[5] Department of Physics, Northwest University, Kano, Nigeria

Email Address

sabiusaid1@yahoo.com (Sabiu Said Abdullahi), suleiman_abdussalam@yahoo.com (Abdussalam B. Suleiman), yukselkoseoglu@sdu.edu.tr (Yuksel Koseoglu), ysdanfari@yahoo.com (Yusuf Shehu), celaliddindurmaz@gmail.com (Yasin Celaleddin Durmaz), baffapet@yahoo.com (Ibrahim M. Musa), hmasud90@yahoo.com (Haidar Masud Alfanda)
*Correspondence: sabiusaid1@yahoo.com

Received: 15 December 2017**; Accepted:** 9 March 2018**; Published:** 20 March 2018

Abstract:

$TM_{0.15}Co_{0.1}Zn_{0.75}O$ nanoparticles with (TM=Ni and Mn) has been successfully synthesized by microwave assisted combustion synthesis method using urea as a fuel. The structural, morphological, compositional and Magnetic properties of these nanoparticles were investigated by X-ray Diffraction Machine (XRD), Scanning Electron Microscopes (FE-SEM JEOL-7001), Energy-Dispersive X-ray Spectroscopy (EDX), and Quantum Design Vibrating Sample Magnetometre (QD-VSM) respectively. The structural properties of both sample showed the formation of Wurtzite structure of ZnO, with nine prominent peaks in which the strong diffraction peaks appear in (100), (002) and (101), respectively, though there is a trace related to the Ni ions observed in the Ni samples. The average sizes of the nanoparticles were estimated using Debye-Scherrer's equation. There is an increase in the average size between 32.65-34.23nm for Ni ion and a decrease in the size from 32.65-25.71nm for Mn ion. Scanning Electron Microscopes (SEM) showed that smaller crystallites of both samples have sizes smaller than 100nm, no indication of phase separation and little agglomeration was observed. Energy-dispersive X-ray Spectroscopy (EDX) confirmed that all the chemical composition of the samples tallies with the synthesis results. Moreover Magnetic measurement reveal that both samples exhibit a room temperature ferromagnetism though its higher in the sample doped by Ni ions.

Keywords:

Nanoparticles, Zinc Oxide, Dilute Magnetic Semiconductor, Combustion Synthesis Method, Ferromagnetism

1. Introduction

Considerable effort has been devoted to Dilute Magnetic Semiconductor (DMS) due to their promising applications in spintronic as microelectronic technology [1] this is as a result of their ability to use spin degrees of freedom and charge manipulation,[2] these makes them attractive to be worked as functionality of memory, detectors [3], light-emitting sources, spin-valve transistors, spin light-emitting diodes, [4] non-volatile storage, logic devices [5] and also used as ultra-fast optical switches or even quantum computing devices[6]. The greatest challenge for these DMSs materials is their ability to retain their magnetic character at room temperature so as to offer the above mentioned technological applications. [7]. As theoretically predicted for the ferromagnetic exchange coupling that, an ideal DMS should have a homogeneous distribution of the magnetic dopants, so the presence of any magnetic precipitate in the host semiconductors in form of secondary phases of the magnetic impurities is detrimental to the real applications of DMSs and therefore should be avoided [8]. However, recent discovery of an experimental result shows that room temperature ferromagnetic materials (RTFM) can be observed when doped with transition metal (TM) that is why worldwide research is triggered on them [9]. In which magnetic ions are employed as a substituent to a small percentage metallic ions in the parent semiconductor materials thereby hosting sp transition metal in the dilute magnetic semiconductors [10]. Among the dilute magnetic semiconductors Zinc Oxide dilute magnetic semiconductor emerge to be the best applicant because of its wide band gap of 3.37 eV and large exciting binding energy of approximately 60meV at 300 K.[6],[11].With these exceptional and interesting properties a number of research was focused on. More attention is given to some novel transition metal elements (Ni, Fe, Mn,Cu Co, V,) doped ZnO DMSs.[12]. It has been reported by Koseoglu Y that $Co_{0.2}Zn_{0.8}O$ sample is found to exhibit a clear RT ferromagnetism with a large coercivity of 560Oe [13]. Mohapatra presented an observation of ferromagnetism in 3% and 5% Co doped ZnO system. He attributed presence of oxygen defects in lower percentage of Co doped ZnO ($\leq$5%) as factor that enhances the carrier mediated exchange interaction thereby enhancing the room-temperature ferromagnetic behavior. However as he predicted that higher doping percentage of cobalt (>5%) creates weak link between the grains and suppresses the carrier mediated exchange interaction consequently room temperature ferromagnetism is not observed in 7% and 10% Co doped ZnO [14]. Glaspel et al. also reported a paramagnetic behavior of 10% Co doped ZnO sample although room temperature ferromagnetism was observed by hydrogenating the samples at 573K for 6h [15]. Meanwhile with observation from Kaushik et al predicted that up to an optimum of 10% Co doped ZnO nanocrystals exhibits room temperature ferromagnetism and the ferromagnetic ordering is strengthening with increasing the Co concentration, further increment of Co concentration decrease the magnetization of the samples, his observation is related to BMP enhanced ferromagnetism, which occur due to the formation of defects, such as oxygen vacancy and Zn interstitials [16]. Sharma et al synthesized $Zn_{1-x}Co_xO$ (x=0.02, 0.05and 0.10) and presented RTFM with larger values of M_S was observed for the samples synthesized with carrier gases (O_2, Ar N_2) [7]. Jianlong et al reported an observation of a room-temperature ferromagnetic property in Co-doped ZnO particles which he probably articulate it from the Co^{3+} enrichment on the particle surface and the coexistence of Co^{2+}/Co^{3+} in the particle, that may lead to the super-exchange or a double-exchange mechanism between the $Co^{2+}$and Co^{3+}[17]. Similar observation was made for other transition metals like Mn

as Junhao reported the display of room-temperature ferromagnetism as well as paramagnetism, in 2.5% and 5% Mn-doped ZnO samples while the 10% and 15% samples exhibit paramagnetic effects. The observed ferromagnetic behaviors likely originate from cooperative effect of intrinsic and extrinsic magnetisms [2]. this coincide with Cheng observation of the coexistence of Ferromagnetic and paramagnetic behavior in the 5% Mn-doped ZnO sample at room-temperature, which may arise from ferromagnetic exchange interaction as well as small secondary phases while the 20% and 40% Mn-doped samples show large paramagnetic effects at room temperature, which is probably due to small paramagnetic secondary phases and clustering of Mn in the samples [8]. Omri et al characterized his samples with 1% and 5% Mn concentrations whereby the former reveal diamagnetic behavior and the latter present both paramagnetic and ferromagnetic behavior. The room ferromagnetic component is due to the presence of the secondary phase $ZnOMn^3$ which is confirmed by his XRD study [12]. Interestingly co doping process are now involved to enhance the magnetic ordering and better optical and magnetic properties of the nanoparticles.[18] Siddheswaran et al. reported that Co, Al co-doped ZnO nanopowders calcined at 600C exhibit the room temperature ferromagnetism and it increases with Co concentration. Conversely, the sintered (1000C) materials display a perfect paramagnetic nature. The defects such as O and Zn vacancies and interstitials are considered to be responsible for the observed ferromagnetism [19]. Abdullahi et al reported an observation of room temperature ferromagnetic behavior with coercive field and remanent magnetization of 47.70 Oe and 1.8×10^{-1} emu/g, in 15% Mn of $Mn_xCo_{0.1}Zn_{0.9-x}O$ nanoparticles [18]. In this paper we utilized Ni and Mn co doped CoZnO nanoparticles as in the formula ($TM_{0.15}Co_{0.1}Zn_{0.75}O$), the structural, and magnetic properties of the samples were investigated.

2. Synthesis

ZnO nanostructured materials were prepared followed by $TM_xCo_{0.1}Zn_{0.9-x}O$ with (TM= Ni and Mn) and x=0.00 to 0.15, These molar ratio of both Nickel (II) nitrate hexa hydrate ($Ni(NO_3)_2.6H_2O$), and Manganese (II) nitrate tetra hydrate ($Mn(NO_3)_2$ ($4H_2O$), was mixed with an appropriate ratio of Cobalt(II) nitrate hexahydrate ($Co(NO_3)_2.6H_2O$) and Zinc nitrate hexahydrate ($Zn(NO_3)2.6H_2O$) respectively as in table 1 were dissolved in 10 mL of doubly distilled water, using urea as a fuel, the mixture is stirred with a magnetic stirrer until it dissolved completely. Then it was poured into a crucible which was taken in to a kitchen type microwave oven that operates with 800 watts for 15 minutes. The solution boil and dehydrates followed by combustion resulting from the evolution of gas in the form of spark. Then the solution burns completely with the release of much amount of heat and gas, where by obtained the desired solid phase.

Table 1. *Amounts of Metal Nitrates Used to Synthesize $TM_{0.15}Co_{0.1}Zn_{0.75}O$ Nanopowders.*

Sample	Ni(II)nitrate (g)	Mn(II)nitrate (g)	Co(II)nitrate (g)	Zn(II)nitrate (g)	Urea (g)
X=0.00	0.000	0.000	0.000	5.940	6.00
X=0.05	0.291	0.000	0.582	5.049	6.00
X=0.05	0.000	0.251	0.582	5.049	6.00
X=0.15	0.872	0.000	0.582	4.455	6.00
X=0.15	0.000	0.753	0.582	4.455	6.00

3. Results and Discussion

3.1. XRD Measurement

Structural characterization of the samples was carried out using Rigaku X-raydiffraction (XRD) spectrometer, Figure 1 shows the combined XRD patterns taken from all the samples. The diffraction patterns indicate wurtzite structure of ZnO where all the diffraction peaks can be pointed out to the hexagonal phase ZnO as reported in JCPDS card (No. 36-1451, a = 0.3249 nm, c = 0.5206 nm) with nine prominent peaks 100, 002, 101, 102,110,103,200,112, and 201. Where the strong diffraction peaks appear in (100), (002) and (101), respectively [20][21]. For the Mn ions there is no any secondary phase observe, However there is a trace or single peak level X observed from the Ni ion in the samples, which is likely to be NiO, the peak increase with the increase in the dopant, this implies that not all Ni ions can substitute Zn^{2+} without changing the structure [22][23].

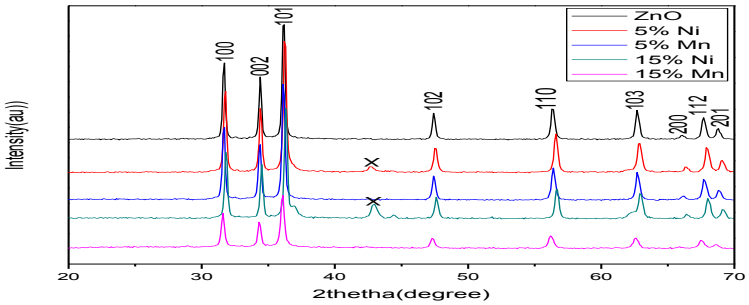

Figure 1. *XRD patterns for $TM_xCo_{0.1}Zn_{0.9-x}O$.*

In finding the sizes of the particles we used Scherrer equation written as [10].

$$D = \frac{k\lambda}{\beta cos\theta} \tag{1}$$

Where, D is the grain size, *K* is a dimensionless shape factor with a value (0.9) which varies with the actual shape of the crystallite, is the wavelength of the X-ray used (1.5402A) . is the full width of the half maximum of the most intense peak, θ is the Bragg angle corresponding to maximum X-ray diffraction peak.[3][16][24]

The calculation of the lattice constant a and c can be done by using the formula for hexagonal system as.

$$\frac{1}{d^2} = \frac{4}{3}\left(\frac{h^2+hk+k^2}{a^2}\right)+\frac{l^2}{c^2} \tag{2}$$

Using Bragg's law we can rewrite the above equation as follows

$$\frac{4sin^2\theta}{\lambda} = \frac{4}{3}\left(\frac{h^2+hk+k^2}{a^2}\right)+\frac{l^2}{c^2} \tag{3}$$

Where *d* is the lattice spacing, *a* and *c* are lattice constants, *hkl* are miller indices. To calculate *a*, we used the peak of the form (hk0) so that *c* will vanish in the equation, similarly to get *c* we used the peak of the form (00l) so that we have only *c* and *l* as our variable. The equation derived for *a* and *c* are respectively given as [21].

$$a = \frac{\lambda\sqrt{(h^2+hk+k^2)}}{\sqrt{3}sin\theta} \tag{4}$$

$$c = \frac{\lambda l}{2sin\theta} \tag{5}$$

Table 2. Particles size and Lattice parameters of $TM_xCo_{0.1}Zn_{0.9-x}O$ Nanoparticles.

Sample	D(101)nm	a (11 0)nm	c (002)nm
ZnO	32.65	3.2614	5. 2085
$Ni_{0.05}Co_{0.1}Zn_{0.85}O$	31.88	3.2503	5.2107
$Mn_{0.05}Co_{0.1}Zn_{0.85}O$	31.29	3.2610	5.2084
$Ni_{0.15}Co_{0.1}Zn_{0.75}O$	34.23	3.2452	5.2000
$Mn_{0.15}Co_{0.1}Zn_{0.75}O$	25.71	3.2631	5.2143

The crystallite sizes of all samples were calculated with Scherrer's equation using the most intense peak (101), the crystal size varies from one dopant to another, for Ni ion it increases from 32.65-34.23nm as a while for Mn ions decrease from 32.65nm to 25.71 as shown in Table 2. which indicates that addition of Ni^{2+}create lattice distortion in the ZnO crystal thereby shifting the diffraction peaks to larger angle eventually reduce the crystallity of the sample [4]. However for Mn ions the growth of the parent compound has been suppressed as a result of the strain induced by the dopant that ultimately reduce the intensity of the diffraction peak and increase its width [12].

Moreover, the lattice parameters *a* and *c* decreases with an increase in Ni ions content and increases with Mn ion. These results from the difference in the ionic radii of Ni^{2+}, and Mn^{2+} with 64 and 80pm respectively. Where the ionic radius of the Ni^{2+} is less than that of Zn^{2+} while that of Mn^{2+} is greater than that of Zn^{2+} these account for the difference in their lattice parameter [19][25].

3.2. SEM Measurement

SEM images reveals that all samples consist of almost spherical shaped nanoparticles, no any indication of phase separation and little agglomeration was observed in all samples only that Mn doped sample shows higher porosity compare to Ni ions, the porosity is related to evolution of gases like Co_2, N_2 and water vapor during the synthesis [26]. A close view of all sample shows that smaller crystallites have sizes smaller than 100nm which confirm the XRD result. This result is similar to that reported by Shanmugam [29]. Moreover, the nanoparticles were dense and distributed evenly on the whole area however, a clear distinct boundary between neighboring crystallites can still be observed [9]. The FE-SEM images of all samples are shown in Figure 2.

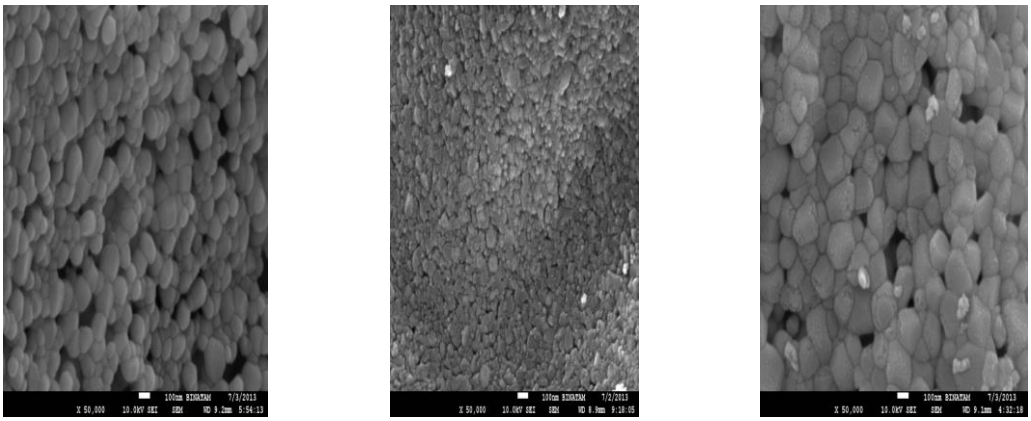

(a) $Zn_{0.85}O$ *(b) $Ni_{0.15}Co_{0.1}Zn_{0.75}O$* *(c) $Mn_{015}Co_{0.1}Zn_{0.75}O$*

Figure 2. Field emission scanning electron micro-graphs (FE-SEM) of $TM_{0.15}Co_{0.1}Zn_{0.75}O$ Nanoparticles.

3.3. EDX Measurement

The EDX measurement results are shown in Fig. 3(a), (b) and (c). The results comply with what is expected from the synthesis where by the mass ratios of the chemical composition of both samples tallies with the outcomes of the EDX spectra. The spectrum contains all the expected elements and no impurity was found.

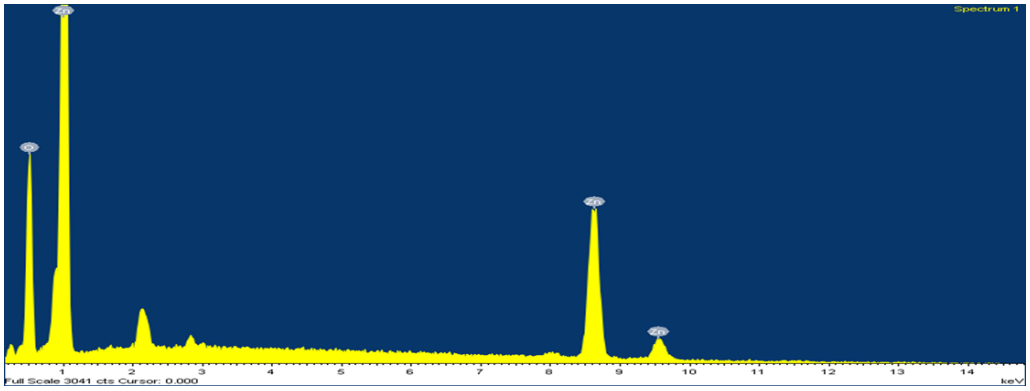

(a) ZnO

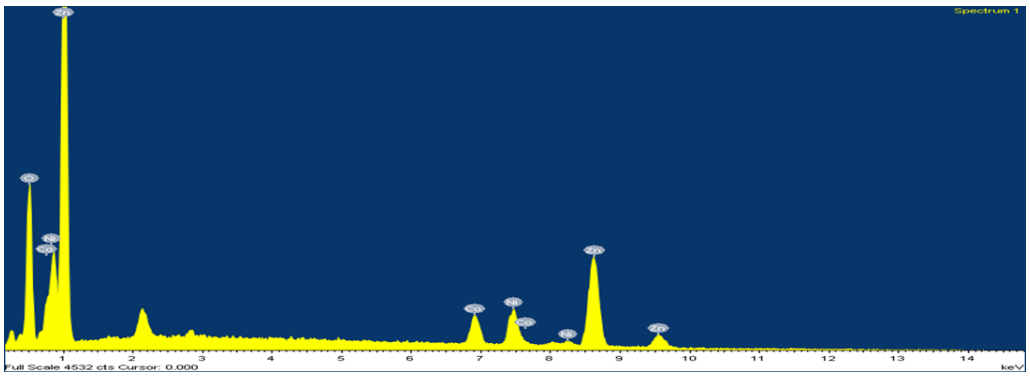

(b) $Ni_{0.15}Co_{0.1}Zn_{0.75}O$

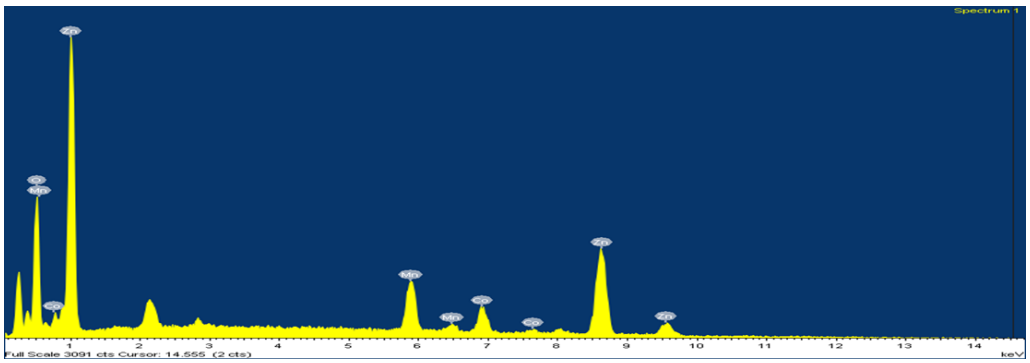

(c) $Mn_{0.15}Co_{0.1}Zn_{0.75}O$

Figure 3(a), (b) and (c). *EDX graph of $TM_{0.15}Co_{0.1}Zn_{0.75}O$ Nanoparticles.*

Table 3. *Elemental Percentage for $TM_{0.15}Co_{0.1}Zn_{0.75}O$ Nanoparticles.*

$Ni_{0.15}Co_{0.1}Zn_{0.75}O$			**$Mn_{0.15}Co_{0.1}Zn_{0.75}O$**		
Element	Weight %	Atomic %	Element	Weight %	Atomic %
O K	8.04	45.79	O K	4.37	49.11
Co K	4.32	6.67	Mn K	3.42	11.21
Ni K	6.83	10.60	Co K	2.69	8.22
Zn L	26.50	36.94	Zn L	11.43	31.47
Total	45.67			21.91	

The spectra of $TM_{0.15}Co_{0.1}Zn_{0.75}O$ nanoparticles are shown in Figure 3. It can be observed that the most abundant element in both samples is Zinc then oxygen followed by the respective element. In both samples the appearance of unnamed peak at almost 2.0eV indicate the presence of carbon atom which result from the carbon coating applied before the EDX measurement [26]. Moreover, from Table 3 the percentage weight of each element is shown which is related with the number of elements in the sample similarly the atomic percentage of oxygen indicates that there is oxygen vacancies in both the sample's only that the vacancy is more presented in Ni ions compared to Mn ions which may result in getting more ferromagnetic behavior of the Ni over the Mn samples. [24].

3.4. Magnetic Measurement

Magnetic measurements were carried out by Quantum Design Magnetometer (QD-VSM). The samples were cooled either in the presence of an external magnetic field (Field cooling case -FC) or in zero fields (zero field cooling case ZFC). The magnetic behaviors were recorded by sweeping the external field between ±10kOe at different temperature. Fig.4 shows the magnetic properties of the samples. It reveals that both samples present room temperature ferromagnetic behavior with a clear S shape hysteresis loops. $Ni_{0.15}Co_{0.1}Zn_{0.75}O$ samples present more ferromagnetic behavior at room temperature when compared with the sample doped with Mn, the latter is observed to have saturation magnetization M_s of 1458emu/g,e coercive field H_c of 146Oe and remanence magnetization of M_r of $2.314x10^{-1}$emu/g which is higher than that of $Mn_{0.15}Co_{0.1}Zn_{0.75}O$ sample with the saturation magnetization of 413.7emu/g, coercive field of 47.70 and remanence magnetization of $1.8x10^{-1}$emu/g as presented in table 4. However room temperature ferromagnetism is observed in both the samples. The presence of room temperature ferromagnetism in $Mn_{0.15}Co_{0.1}Zn_{0.75}O$ can be proven from FC and ZFC as in Fig.5(b). İt is clearly shown that the curie temperature (TC) is above room temperature since the field diverges at 295K [27] [28]. Similar results were obtain from the literature as Jiang reported the Coercivity Hc and saturation magnetization of 120Oe and 0.002emu/g in the 5% Mn doped ZnO nanoparticles prepared by Sol gel method [2]. Koseoglu reported an observation of ferromagnetic behavior in Ni doped ZnO nanoparticle prepared by Microwave assisted combustion method with coercivity value of 335Oe for the 5% sample. [25]. Room temperature magnetic behavior was observed by Vijayaparasath with 20% Ni and Mn doped ZnO nanoparticles with saturation magnetization varies from 0.18-0.883emu/g [30]. A solid state reaction route was used to observe a clear hysteresis loops as a function of the magnetic field for 2% Mn doped ZnOwith the coercive value of 193G and saturation magnetization of 28.54 x 10^{-3} emu/g [31]. However Mohapatra reported higher coercive value for the Co doped ZnO samples with 970Oe and 1033Oe in 3 and 5% Samples respectively [14]. Also Room temperature Ferromagnetism was Observed by Wu et al. in 10 and 20% Fe doped ZnO nanoparticles by hydrothermal method with the coercivity and saturation magnetization of 90Oe, 78Oe and 0.74emu/g, 01.74 respectively [32].

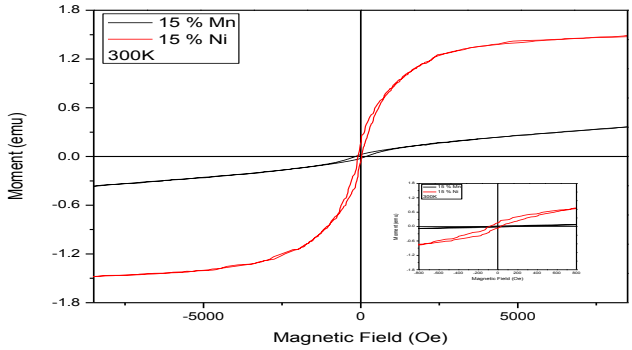

Figure 4. *M–H curve of $TM_{0.15}Co_{0.1}Zn_{0.75}O$ Nanoparticles for both samples.*

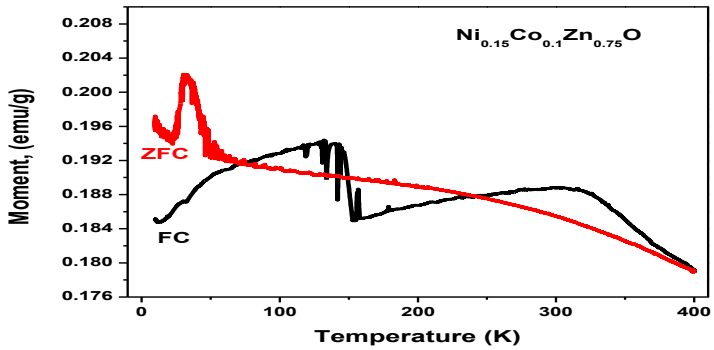

Figure 5(a). *Zero Field Cooling (ZFC) and Field Cooling (FC) at room temperature for $Ni_{0.15}Co_{0.1}Zn_{0.75}O$ Nanoparticles.*

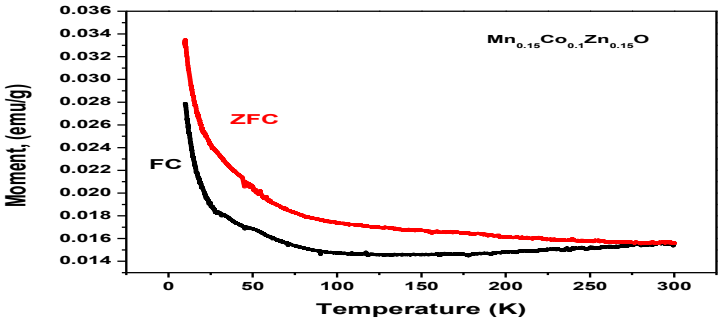

Figure 5(b). *Zero Field Cooling (ZFC) and Field Cooling (FC) at room temperature for $Mn_{0.15}Co_{0.1}Zn_{0.75}O$ Nanoparticles.*

Table 4. *Magnetic measurement of the $TM_{0.15}Co_{0.1}Zn_{0.75}O$ Nanoparticles.*

Samples	M_s (emu/g)	H_c (Oe)	M_r (emu/g)
$Ni_{0.15}Co_{0.1}Zn_{0.75}O$	1458	146.0	$2.314x10^{-1}$
$Mn_{0.15}Co_{0.1}Zn_{0.75}O$	413.7	47.70	1.8×10^{-1}

Research have shown that the ferromagnetic behavior is normally attributed to certain factors, (1) the intrinsic property of the sample such that the exchange interaction between free delocalized carriers coming from the oxygen vacancies, zinc interstitials or from the localized d spins on the dopant ions may result from room temperature ferromagnetism [14] [5]. or (2) due to presence of secondary phase that act as a defect in the parent compound [14][2]. The room temperature ferromagnetism

observed from $Ni_{0.15}Co_{0.1}Zn_{0.75}O$ is possibly originated from both the oxygen vacancy and formation of NiO as a secondary phase in the samples structure as observed in the XRD measurement. This may account for the additional ferromagnetic behavior in $Ni_{0.15}Co_{0.1}Zn_{0.75}O$ sample and hence present higher room temperature ferromagnetism compared to $Mn_{0.15}Co_{0.1}Zn_{0.75}O$ samples.

4. Conclusions

We have successfully synthesized $TM_xCo_{0.1}Zn0._{9-x}O$ nanoparticles with (TM= Ni and Mn) by microwave assisted combustion synthesis method using urea as a fuel. The structural, properties showed the formation of Wurtzite structure of ZnO with nine prominent peaks meanwhile there is a formation of secondary phasee observed in the sample doped with Ni ions. The average size of the nanoparticles increases with Ni dopant while decreases for the Mn dopant. Scanning Electron Microscopes (SEM) of both samples showed that smaller crystallites have sizes smaller than 100nm, Magnetic measurement reveal that both samples exhibit a room temperature ferromagnetic behavior However, the behavior is higher in the sample doped with Ni ion when compared to Mn ion. The saturation magnetization $M_{s,}$ coercive field $H_{c,}$ and remanence magnetizations of 1458emu/g, 146Oe $2.314x10^{-1}$emu/g and 413.7emu/g, 47.70, $1.8x10^{-1}$emu/g respectively.

Conflicts of Interest

The authors declare that there is no conflict of interest regarding the publication of this article

Acknowledgments

The Author acknowledges Kano State Government under the leadership of Engr. Rabiu Musa Kwankwaso for their support toward my master degree.

References

[1] M.V. Limaye; S.B. Singh; R. Das; P. Poddar; S.K. Kulkarni. Room temperature ferromagnetism in undoped and Fe doped ZnO nanorods : Microwave-assisted synthesis. *J. Solid State Chem*. 2011, 184(2), 391-400.

[2] Y. Jiang; W. Wang; C. Jing; C. Cao; J. Chu. Sol - gel synthesis, structure and magnetic properties of Mn-doped ZnO diluted magnetic semiconductors," Mater. Sci. Eng. B, 2011, 176(16), 1301-1306.

[3] S. Chattopadhyay; S. Dutta; A. Banerjee; D. Jana; S. Bandyopadhyay; S. Chattopadhyay; A. Sarkar. Synthesis and characterization of single-phase Mn-doped ZnO. 2009, 404, 1509-1514.

[4] Y. Caglar. Sol - gel derived nanostructure undoped and cobalt doped ZnO : Structural, optical and electrical studies. *J. Alloys Compd.* 2013, 560, 181-188.

[5] S.K. Mandal; T.K. Nath. Microstructural, magnetic and optical properties of ZnO : Mn ($0.01 \leq x \leq 0.25$) Epitaxial diluted magnetic semiconducting films. *Thin Solid Films.* 2006, 515, 2535-2541.

[6] J.F. Fern; A.C. Caballero; M. Villegas; S.J. Khatib; M.A. Ba; J.L.G. Fierro; J.L. Costa-kramer; E. Lopez-ponce; M.S. Mart. Structure and magnetism in the Zn –

Mn – O system : A candidate for room temperature ferromagnetic semiconductor. 2006, 26, 3017-3025.

[7] V.K. Sharma; M. Najim; A.K. Srivastava; G.D. Varma. Structural and magnetic studies on transition metal (Mn , Co) doped ZnO nanoparticles. *J. Magn. Magn. Mater.* 2012, 324(5), 683-689.

[8] C. Jing; Y. Jiang; W. Bai; J. Chu; A. Liu. Synthesis of Mn-doped ZnO diluted magnetic semiconductors in the presence of ethyl acetoacetate under solvothermal conditions. *J. Magn. Magn. Mater.* 2010, 322(16), 2395-2400,.

[9] Y. Koseoglu. Structural, magnetic, electrical and dielectric properties of MnxNi 1-x Fe 2O4 spinel nanoferrites prepared by PEG assisted hydrothermal method. *ceramic international*, 2013, 39, 4221-4230.

[10] Y. Koseglu; F. Alan; M. Tan; R. Yilgin. Low temperature hydrothermal synthesis and characterization of Mn doped cobalt ferrite nanoparticles. 2012, 38, 3625-3634.

[11] S.S. Abdullahi; Y. Koseoglu; C.E. Ndikilar; A.A. Safana; S. Ahmad. Effect of Cu and Co Doping on the structural properties of ZnO nanoparticles. *journal of the Nigerian assosiation of Mathematical Physics*, 2015, 30, 443-448.

[12] K. Omri; J. El Ghoul; O.M. Lemine; M. Bououdina; B. Zhang; L. El Mir. Magnetic and optical properties of manganese doped ZnO nanoparticles synthesized by sol – gel technique. *Superlattices Microstruct.* 2013, 60,139-147.

[13] Y. Koseoglu. Enhanced Ferromagnetic Properties of Co-doped ZnO DMS Nanoparticles. *Suppercond.* 2013, 485-489.

[14] J. Mohapatra; D.K. Mishra; D. Mishra; A. Perumal; V.R.R. Medicherla; D.M. Phase; S.K. Singh. Room temperature ferromagnetism in Co doped ZnO within an optimal doping level of 5 %. *Mater. Res. Bull.* 2012, 47(6), 1417-1422.

[15] G. Glaspell; P. Dutta; A. Manivannan. A Room-Temperature and Microwave Synthesis of M-Doped ZnO (M = Co, Cr , Fe , Mn & Ni). *Journal of Cluster Science*, 2005, 16(4), 523-536.

[16] A. Kaushik; B. Dalela; R. Rathore; V.S. Vats; B.L. Choudhary; P.A. Alvi; S. Kumar; S. Dalela. Influence of Co doping on the structural, optical and magnetic properties of ZnO nanocrystals. *J. Alloys Compd.* 2013, 578, 328-335.

[17] J. Fu; X. Re-n; S. Yan; Y. Gong; Y. Tan; K. Liang; R. Du; X. Xing; G. Mo; Z. Chen; Q. Cai; D. Sun; Z. Wu. Synthesis and structural characterization of ZnO doped with Co : Impurity. *J. Alloys Compd.* 2013, 558, 212-221.

[18] S.S. Abdullahi; Y. Koseoglu.; et al. Synthesis and characterization of Mn and Co codoped ZnO nanoparticles. *Superlattice and microstructure*, 2015, 83, 342-352.

[19] R. Siddheswaran; R.V. Mangalaraja; M. Elana; R.E. Avila; C.E. Jeyanthi. Room temperature ferromagnetism in combustion synthesized nanocrystalline Co, Al co-doped ZnO. *J. Alloys Compd.* 2013, 581, 146-149.

[20] O.D. Jayakumar; I.K. Gopalakrishnan; C. Sudakar; S.K. Kulshreshtha. Synthesis of manganese doped ZnO single crystals and their magnetization studies. *Journal of Crystal Growth*, 2006, 294(2), 432-436.

[21] Z. Pan; X. Tian; S. Wu; X. Yu; Z. Li; J. Deng; C. Xiao; G. Hu; Z. Wei. Investigation of structural, optical and electronic properties in Al – Sn co-doped ZnO thin films. *Appl. Surf. Sci.* 2013, 265, 870-877.

[22] S. Khatoon; T. Ahmad. Synthesis, Optical and Magnetic Properties of Ni-Doped ZnO Nanoparticles. *Carbon - Science and Technology*, 2012, 2(6), 325-333.

[23] K. Vallalperuman; M. Parthibavarman; S. Sathishkumar; M. Durairaj; K. Thavamani. Synthesis and characterization of Co and Mn doped NiO nanoparticles. *Korean Journal of Chemical Engineering*, 2014, 31(4), 639-643.

[24] Sharma, P.; Gupta, A.; Rao K.V.; Owens F.J. Origion of ferromagnetism in thin film and nanoparticles of inorganic materials, Natural. *Material,* 2003, 2, 673.

[25] Y. Köseoğlua; Y.C. Durmaza; R.Yilgin. Rapid synthesis and room temperature ferromagnetism of Ni doped ZnO DMS nanoflakes. *Ceramics International*. 2014, 40, 10685-10691.

[26] Y. Köseoğlu. Fuel aided rapid synthesis and room temperature ferromagnetism of M0.1Co0.1Zn0.8O (M= Mn, Ni, Fe and Cu) DMS Nanoparticles. *Ceramics International.* 2016, 42, 9190-9195.

[27] R.N. Ajwafi. Surface defect mediated magnetic interactions and ferromagnetism in Cr/Co Co-doped ZnO nanoparticles. *J. Magn. Magn. Mater*. 2013, 332, 130-136.

[28] T. Nguyen, V. Canhi. Synthesis of undoped M-doped ZnO (M = Co, Mn) nanopowder in water using microwave irradiation. *J. Phys. Conf. Ser.* 187, p. 012020 2009

[29] N. Shanmugam; K. Dhanaraj; G. Viruthagiri; K. Balamurugan; K. Deivan. Synthesis and Characterization of surfactant assisted Mn^{2+} doped ZnO nanocrystals. *Arabian Journal of Chemistry*, 2016, 9, S758-S764.

[30] G. Vijayaparasath; R. Murugan; S. Asaithambi; P. Sakthivel; T. Mahalingam; G. Ravi. Structural and Magnetic Properties of Ni/Mn Codoped ZnO nanoparticles. AIP Conference Proceeding, 1728, 020650 2016, DOI: 10.1063/1.4946701.

[31] S.A. Ahmed. Structural Optical and Magnetic properties of Mn doped ZnO Samples. *Results in Physics*, 2017, 7, 604-610.

[32] W. Xianojuan; W. Zhiqiang; Z. Lingling; W. Xuan; Y. Hua; J. Jinlong. Optical and magnetic properties of Fe Doped ZnO nanoparticles obtained by Hydrothermal synthesis. *Journal of nanomaterials*, 2014, 2014, 1-6.